HHS Public Access

Author manuscript

*Langmuir*. Author manuscript; available in PMC 2022 June 29.

Published in final edited form as:

*Langmuir*. 2021 June 29; 37(25): 7780–7788. doi:10.1021/acs.langmuir.1c01018.

# A Solid-State NMR Study to Probe the Effects of Divalent Metal Ions ($Ca^{2+}$ and $Mg^{2+}$) on the Magnetic-Alignment of Polymer Based Lipid-Nanodiscs

**Thirupathi Ravula**[a,‡], **Xiaofeng Dai**[a,b,‡], **Ayyalusamy Ramamoorthy**[a,*]

[a]Biophysics Program and Department of Chemistry, Biomedical Engineering, and Macromolecular Science and Engineering, The University of Michigan, Ann Arbor, MI 48109-1055, USA

[b]Xiaofeng Dai was a visiting student from the College of Chemistry, Nankai University, Tianjin 300071, China.

## Abstract

Divalent cations, especially $Ca^{2+}$ and $Mg^{2+}$, play a vital role on the function of biomolecules and thus making them important to be contained in the samples for in-vitro biophysical and biochemical characterizations. While lipid nanodiscs are becoming valuable tools for structural biology studies on membrane proteins and for drug delivery, most types of nanodiscs used in these studies are unstable in the presence of divalent metal ions. To avoid the interaction of divalent metal ions with the belt of the nanodiscs, synthetic polymers have been designed and demonstrated to form stable lipid-nanodiscs under these conditions. Such polymer-based nanodiscs have been shown to provide an ideal platform for structural studies using both solid-state and solution NMR spectroscopy because of the near-native cell-membrane environment they provide and the unique magnetic-alignment behavior of large-size nanodiscs. In this study, we report an investigation probing the effects of $Ca^{2+}$ and $Mg^{2+}$ ions on the formation of polymer-based lipid-nanodiscs, and on the magnetic-alignment properties using a synthetic polymer, SMA-QA, and DMPC lipids. Phosphorus-31 NMR experiments were used to evaluate the stability of the magnetic-alignment behavior of the nanodiscs for varying concentrations of $Ca^{2+}$ or $Mg^{2+}$ at different temperatures. It is remarkable that the interaction of divalent cations with lipid headgroups promotes the stacking up of nanodiscs that result in enhanced magnetic-alignment of nanodiscs. Interestingly, the reported results show that both temperature and concentration of divalent metal ions can be optimized to achieve optimal alignment of nanodiscs in the presence of an applied magnetic field. We expect the reported results to be useful in the design of nanodiscs based nanoparticles for various applications in addition to atomic-resolution structural and dynamics studies using NMR and other biophysical techniques.

## Graphical Abstract

*Corresponding Author: ramamoor@umich.edu.

Author Contributions

The manuscript was written through contributions from all authors. All authors have given approval to the final version of the manuscript.

‡These authors contributed equally to this study.

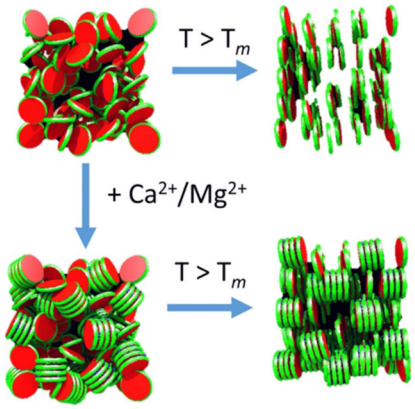


Although detergents are still used in the structural studies of membrane proteins, native-like membrane mimetics are essential to functionally reconstitute and investigate the structure, dynamics, and function of membrane-associated proteins. Among the many types of membrane mimetics, lipid-nanodiscs are increasingly used in the biophysical and biochemical studies. The belt surrounding the lipid bilayer in a nanodisc is made up of amphipathic membrane scaffold proteins (MSP),[1–9] short amphipathic peptides[10–13] or synthetic amphipathic polymers.[14–16] These different types of belts have their own advantages and limitations. Among them, synthetic polymers are gaining more attention due to their ability to directly extract membrane proteins from cell lysates without the use of detergents and the feasibility to functionalize the polymer with chemical groups as desired.[14] Recent studies have demonstrated the nanodisc formation by a variety of polymers that are cationic,[17–20] anionic,[15, 21–23] zwitterionic,[24] styrene-containing, styrene-free,[19, 22–23] charge-free, and metal-chelators.[25] Some of these polymers have been shown to be stable against pH and some of them can be used to form nanodiscs for certain pH values.[17–18, 20, 26] This library of amphipathic polymers have significantly expanded the applications of nanodiscs.[27–43]

One of the limitations of many of the polymer based nanodiscs is their instability against divalent metal ions, for example $Ca^{2+}$ and $Mg^{2+}$. But, $Ca^{2+}$ and $Mg^{2+}$ are two of the most important cations present in human body, which are critical for the function of a variety of biomolecules.[44–49] For example, a concentration of 1–10 mM $Mg^{2+}$ is essential for some of the RNAs to fold and for the ribozyme activities.[50] There are also proteins that require divalent cations for their activities; for example, $Ca^{2+}$ dependent calmodulin and other proteins, and $Mg^{2+}$ dependent bovine heart glycogen synthase D and glucose-6-phosphate dehydrogenase enzyme.[51–52] The concentration of divalent cations can also influence the membrane binding, folding, structure and membrane orientation of membrane proteins such as phospholamban and the annexins.[53–56] Because of these reasons, it is important to make sure that the membrane mimetics are tolerant to the presence of divalent metal ions.

Recent studies have been successful in designing synthetic polymers and demonstrating their application to form stable nanodiscs against divalent metal ions. Since the size of the polymer-based nanodiscs can be varied by simply changing the lipid:polymer ratio, it is feasible to prepare very large-size nanodiscs called ‘macro-nanodiscs’ (>20

nm in diameter) as demonstrated in the literature.[21, 57] Such macro-nanodiscs have been shown to spontaneously align in the presence of an external magnetic field with its lipid-bilayer-normal oriented perpendicular to the magnetic field direction.[21, 57] In addition, the alignment axis can be flipped by 90° to render the lipid-bilayer-normal to orient along the magnetic field axis by using paramagnetic ions as demonstrated in the literature.[21, 26, 58–59] The ability to align, and flip the alignment axis, enables the measurement of anisotropic NMR parameters such as chemical shift anisotropy, dipole-dipole couplings, and quadrupole couplings for solid-state NMR experiments. Such static solid-state NMR experiments have been well developed for the structural studies of a variety of membrane-associated proteins.[21, 57, 60–61] Similar to other alignment media used in the biomolecular NMR studies,[62–65] the 'macro-nanodiscs' have also been successfully used as an alignment medium to measure residual dipolar couplings (RDCs) by well-established solution NMR experiments.[60] A recent study has demonstrated the feasibility of measuring natural-abundance $^{17}O$ residual-quadrupole coupling of water molecules that are dynamically associated with lipid-nanodiscs.[61] While the polymer-based nanodiscs can be useful for atomic-resolution studies on membrane proteins, not all of the polymers that can form nanodiscs are stable against the divalent metal ions. For example, the nanodiscs forming SMA-EA,[21] SMA-dA,[18] and PAA[23] precipitate at high concentrations of divalent metal ions as they contain carboxyl groups that can chelate with metals resulting in the instability. On the other hand, the nanodiscs forming SMA-QA[20] and PMA[19] polymers are stable against high concentrations of divalent metal ions.

While the absence of metal-chelating groups in the positively charged polymers, SMA-QA and PMA, make them stable against divalent metal ions, it is unclear if the interaction of divalent metal ions with lipids contained within the nanodiscs would play any role on the stability and magnetic-alignment properties of the macro-nanodiscs. To address this question, herein we systematically examined the effects of $Ca^{2+}$ and $Mg^{2+}$ on the formation of polymer-based nanodiscs and on the magnetic-alignment properties using a synthetic polymer, SMA-QA, and DMPC lipids. A schematic for the chemical structure of SMA-QA and an illustration of a nanodisc are shown in Figure 1. Static phosphorus-31 NMR experiments were used to evaluate the stability of the magnetic-alignment behavior of the nanodiscs for various concentrations of $Ca^{2+}$ and $Mg^{2+}$.

## EXPERIMENTAL SECTION

### Preparation and characterization of polymer-based macro-nanodiscs:

The synthesis, purification, and characterization of amphipathic SMA-QA polymer and its ability to form nanodiscs are described elsewhere.[20, 61] 1,2-dimyristoyl-sn-glycero-3-phosphocholine (DMPC) was purchased in the powder form from Avanti Polar Lipids (Alabama). Lipids were dispersed in 10 mM HEPES buffer with 100 mM NaCl, and then sonicated for 10 min. The polymer was dissolved in the same buffer and mixed with the lipid solution. After three freeze-thaw cycles, the lipid-polymer mixture was incubated at room temperature for 12 h. The clear mixture was then loaded to the column for Size Exclusive Chromatography (SEC), and then purified using 10 mM HEPES buffer and 100 mM NaCl. The SEC profile shown in Figure 1 shows the elution of nanodiscs at 20 ml that

are estimated to have a size of ~25±4 nm diameter as reported in our previous publication[61] and the free polymers elute around 40 ml. We have previously reported on the effect of critical micellar concentration (cmc) on the equilibrium between free- and nanodisc-bound polymers.[66] After concentrating the nanodiscs containing solution to 200 μl, the solution was kept at 4 °C.

### NMR experiments:

Phosphorus-31 NMR experiments were performed on a Bruker solid-state NMR spectrometer operating at 400.11 MHz for $^{1}H$ and 161.96 MHz for $^{31}P$ resonance frequencies. The spectra were acquired as a function of temperature from 295 to 315 K by increasing the sample temperature in steps of 5 K. Upon a change in the temperature, the sample was equilibrated for about 20 min before acquiring NMR data. A solution of $H_3PO_4$ was used as a reference sample and its $^{31}P$ NMR frequency was set to 0 ppm. Other experimental details are provided in the figure captions.

## RESULTS AND DISCUSSION

### Phosphorus-31 NMR reveals the magnetic-alignment of nanodiscs above the main phase transition temperature of lipids

To investigate the effects of lipid interaction with divalent metal ions (such as $Ca^{2+}$ and $Mg^{2+}$), the positively charged SMA-QA polymer was used due to its stability in the presence of these metal ions. Polymer macro-nanodiscs of size ~25±4 nm in diameter were prepared using DMPC lipids and characterized as reported previously.[20, 26, 60–61] $^{31}P$ NMR spectra were recorded to examine the magnetic-alignment of nanodiscs. $^{31}P$ NMR spectra shown in Figure 2 exhibit an isotropic peak at −1 ppm and an anisotropic peak at ~−14 ppm below the phase transition temperature ($T_m$, ~300 K for pure DMPC). The random orientations of the nanodiscs below $T_m$ result in the axially symmetric powder pattern with the perpendicular edge at ~−14 ppm. When the temperature of the sample was increased above the gel-to-liquid-crystalline phase transition temperature (300 K and above), the anisotropic peak position changed to ~−18 ppm and became narrow with an enhanced intensity indicating the magnetic-alignment of nanodiscs. Further increase in the sample temperature (> 300 K), increased the intensity of the anisotropic peak and decreased the isotropic $^{31}P$ NMR peak at −1 ppm.

Linewidth for the anisotropic peak at ~−18 ppm indicating a better alignment of nanodiscs when the constituent lipids are in fluid lamellar phase. On the other hand, the isotropic peak that disappeared at 300 K started to appear and grew in intensity with the increasing temperature indicating the presence of a mixture of both isotropic and aligned nanodiscs. This observation is in agreement with a previously reported results[20] that also showed the stability of nanodiscs against the divalent metal ions based on the static light scattering experiments. The appearance of a peak in the region of ~−14–16 ppm above the phase transition temperature of the lipids indicates the magnetic-alignment of nanodiscs with the bilayer-normal oriented perpendicular to the magnetic field axis as shown previously.[21, 26] For this uniaxial orientation of macro-nanodiscs, $^{31}P$ chemical shift of the motionally-

averaged lipids appear at the perpendicular edge of the chemical shift powder pattern (i.e. ~−13 to 16 ppm), which varies with the sample temperature as shown in Figure 3.

After the successful confirmation of magnetic-alignment of nanodiscs, divalent metal ions were added to the sample to measure the effects of metals on the magnetic-alignment properties of nanodiscs. A series of $^{31}$P NMR spectra of DMPC-SMA-QA macro-nanodiscs were recorded as a function of temperature for the nanodiscs by varying the concentration of metal ions. $^{31}$P NMR spectra obtained in the presence of 10, 20, 35, and 50 mM concentrations of $Ca^{2+}$ ions and $Mg^{2+}$ ions are shown in Figures 2 and 3, respectively. The observed $^{31}$P NMR spectral features can be divided into three types: (i) isotropic peak at −1 ppm, (ii) anisotropic peak in the region of ~−14 to ~−18 ppm due to the magnetic-alignment of nanodiscs that have the lipid-bilayer-normal oriented perpendicular to the direction of the external magnetic field, and (iii) axially symmetric powder pattern appearing as a broad line with a maximum at ~−14 ppm. $^{31}$P NMR spectra recorded at 295 K (i.e. below the phase transition temperature of pure DMPC) showed an axially symmetric powder pattern along with the isotropic peak appearing at ~−1 ppm as explained above for the samples containing no metal ions and also a contribution from aligned nanodiscs. While signal intensities observed for frequencies > 0 ppm are low, simulation was used to disentangle the different contributions as shown in Figure S1 for the spectrum obtained at 295 K with 10 mM $Ca^{2+}$ ions. The isotropic peak indicates the isotropic nature of nanodiscs that tumble fast in the NMR timescale. The combination of isotropic and axially symmetric powder pattern was found to be dependent on the concentration of $Ca^{2+}$. An increase in the concentration of $Ca^{2+}$ ions increased the intensity of isotopic peak; in fact, only the isotropic peak was observed at 50 mM $Ca^{2+}$ (see Figure 2). This effect was found to be more prominent in the presence of $Ca^{2+}$ as compared to $Mg^{2+}$, whereas a combination of powder pattern and isotropic peaks were observed even at 50 mM $Mg^{2+}$ (see Figure 3). For temperatures above $T_m$, the intensities of the anisotropic and isotropic peaks varied depending on the concentration of the metal ions and sample temperature as explained above for samples with no metal ions. In addition, broadening of the aligned peak in the presence of $Ca^{2+}$ and better alignment in the presence of $Mg^{2+}$ ions can be seen from spectra shown in Figures 2 and 3. For example, at 310 K, the intensity of the anisotropic peak increased for 10 and 20 mM $Ca^{2+}$ and decreased for higher concentrations of $Ca^{2+}$ ions (Figure 2). On the other hand, the intensity of the anisotropic peak is higher in the presence of $Mg^{2+}$ ions and did not change significantly with increasing concentration of $Mg^{2+}$ ions for all temperatures above $T_m$ (Figure 3). These results indicate that the degree of alignment and stability of macro-nanodiscs are different for $Ca^{2+}$ and $Mg^{2+}$ ions, with much better alignment in the presence of $Mg^{2+}$ ions which may be attributed to the difference in their binding affinities with lipids.

## Effect of magnesium and calcium cations on $^{31}$P chemical shifts.

Since a divalent metal ion is known to interact with phospholipid head group, the presence of divalent metal ions can alter the observed $^{31}$P chemical shift values. To better understand the chemical shift dependence on the metal ion concentration, the experimentally measured $^{31}$P chemical shift values for the anisotropic peak are plotted in Figure 4 as a function of metal ion concentration and for various sample temperatures (Figure 5). The $^{31}$P chemical

shift of the aligned macro-nanodiscs was found be more negative with increasing $Ca^{2+}$ ion concertation for all the temperatures, whereas it was found to be varying to a lesser extent for $Mg^{2+}$ as shown in Figure 4. These results suggest a stronger binding of $Ca^{2+}$ ions with lipids as compared to $Mg^{2+}$ ions.

To further confirm the effect of metal binding on $^{31}P$ chemical shift, $^{31}P$ NMR experiments were performed on multilamellar vesicles (MLVs) of DMPC (Figure 6). $^{31}P$ NMR spectra were acquired as a function of temperature with varying of $Ca^{2+}$. The frequency of the perpendicular edge of $^{31}P$ CSA powder pattern is shifted to a negative value in the presence of the $Ca^{2+}$ as shown in Figure 6 for multilamellar vesicles. These results further confirm that the observed chemical shift values in the presence of $Ca^{2+}$ ions for macro-nanodiscs (as shown in Figure 4) are indeed due to the binding of $Ca^{2+}$ ions to the lipid head group.

The $^{31}P$ chemical shift values measured as a function of temperature for various concentration of metal ions are shown in Figure 5. The observed chemical shift values vary (decrease) linearly with temperature, which is in good agreement with previous studies on bicelles.[67] The effect is more pronounced for $Ca^{2+}$ ions than that observed in the presence of $Mg^{2+}$ ions as shown in Figure 5. The observed difference in the influence of divalent metal ions on the magnetic-alignment of nanodiscs suggests that the interaction of divalent metal ions with lipid head groups assists the magnetic-alignment of nanodiscs in the lamellar phase of the lipids. This observation could be attributed to the mechanical stacking of nanodiscs in the lamellar phase of the lipids, as illustrated in Figure 7. Overall the reported results are similar to the observations for magnetically-aligned DMPC:DHPC bicelles in the presence of divalent metal ions.[68] Such type of mechanical stacking has been reported for MSP based lipid-nanodiscs in the presence of calcium ions.[69] In addition, such stacking of nanodiscs observed in samples prepared for TEM experiments, where uranyl salts ($UO_2^{2+}$) are used for negative staining, demonstrates the common feature for nanodiscs based on polymer,[22] peptides[70] or protein.[71] It is worthwhile to use divalent metal ions to prepare such stacked nanodiscs for structural studies using cryo-EM and diffraction methods.

In conclusion, this study reports the effects of $Ca^{2+}$ and $Mg^{2+}$ ions on the formation of polymer-based lipid-nanodiscs and on their magnetic-alignment properties. The positively charged amphipathic SMA-QA polymer, that is stable against the divalent metal ions, is used to probe the interaction of $Ca^{2+}$ and $Mg^{2+}$ ions with DMPC lipids. Phosphorus-31 NMR experiments under static conditions were used to evaluate the stability of the magnetic-alignment behavior of the macro-nanodiscs containing various concentrations of $Ca^{2+}$ or $Mg^{2+}$ ions at different temperatures. It is remarkable that the interaction of divalent cations with lipid headgroups promotes the stacking up of macro-nanodiscs that results in the enhanced magnetic-alignment of macro-nanodiscs above the main phase transition temperature of the lipids. Interestingly, the reported results show that both temperature and concentration of divalent metal ions can be optimized to achieve an optimal alignment of nanodiscs. We believe that the reported results would be useful in the design of nanodiscs based nanoparticles for various applications in addition to the structural studies using solid-state and solution NMR techniques. While nanodiscs are used to trap the amyloid intermediates,[40, 72–74] studies investigating the role of metals (such as $Cu^{2+}$, $Zn^{2+}$, $Al^{3+}$ and

other metals) on the amyloid aggregation in a membrane environment would benefit from the use of polymer nanodiscs that are stable against the metal ions.[75–78]

## Supplementary Material

Refer to Web version on PubMed Central for supplementary material.

## Funding Sources:

This research was supported by the National Institute of Health (R35GM139573 to A.R.).

## REFERENCES

1. Denisov IG; Sligar SG, Nanodiscs in Membrane Biochemistry and Biophysics. Chem Rev 2017, 117, 4669–4713. [PubMed: 28177242]
2. Nasr ML; Baptista D; Strauss M; Sun ZJ; Grigoriu S; Huser S; Pluckthun A; Hagn F; Walz T; Hogle JM; Wagner G, Covalently circularized nanodiscs for studying membrane proteins and viral entry. Nat Methods 2017, 14, 49–52. [PubMed: 27869813]
3. Denisov IG; Sligar SG, Nanodiscs in Membrane Biochemistry and Biophysics. Chem. Rev 2017, 117, 4669–4713. [PubMed: 28177242]
4. Denisov IG; Sligar SG, Nanodiscs for structural and functional studies of membrane proteins. Nat. Struct. Mol. Biol 2016, 23, 481–486. [PubMed: 27273631]
5. Nath A; Atkins WM; Sligar SG, Applications of Phospholipid Bilayer Nanodiscs in the Study of Membranes and Membrane Proteins. Biochemistry 2007, 46, 2059–2069. [PubMed: 17263563]
6. Camp T; McLean M; Kato M; Cheruzel L; Sligar S, The hydrodynamic motion of Nanodiscs. Chem Phys Lipids 2019, 220, 28–35. [PubMed: 30802435]
7. Redhair M; Clouser AF; Atkins WM, Hydrogen-deuterium exchange mass spectrometry of membrane proteins in lipid nanodiscs. Chem Phys Lipids 2019, 220, 14–22. [PubMed: 30802434]
8. Hagn F; Nasr ML; Wagner G, Assembly of phospholipid nanodiscs of controlled size for structural studies of membrane proteins by NMR. Nat Protoc 2018, 13, 79–98. [PubMed: 29215632]
9. Padmanabha Das KM; Shih WM; Wagner G; Nasr ML, Large Nanodiscs: A Potential Game Changer in Structural Biology of Membrane Protein Complexes and Virus Entry. Front Bioeng Biotechnol 2020, 8, 539. [PubMed: 32596222]
10. Prade E; Mahajan M; Im SC; Zhang M; Gentry KA; Anantharamaiah GM; Waskell L; Ramamoorthy A, A Minimal Functional Complex of Cytochrome P450 and FBD of Cytochrome P450 Reductase in Nanodiscs. Angew Chem Int Ed Engl 2018, 57, 8458–8462. [PubMed: 29722926]
11. Ravula T; Ishikuro D; Kodera N; Ando T; Anantharamaiah GM; Ramamoorthy A, Real-Time Monitoring of Lipid Exchange via Fusion of Peptide Based Lipid-Nanodiscs. Chem Mater 2018, 30, 3204–3207.
12. Zhang M; Huang R; Ackermann R; Im SC; Waskell L; Schwendeman A; Ramamoorthy A, Reconstitution of the Cytb5-CytP450 Complex in Nanodiscs for Structural Studies Using NMR Spectroscopy. Angew. Chem. Int. Ed 2016, 128, 4497–4499.
13. Salnikov ES; Aisenbrey C; Anantharamaiah GM; Bechinger B, Solid-state NMR structural investigations of peptide-based nanodiscs and of transmembrane helices in bicellar arrangements. Chem Phys Lipids 2019, 219, 58–71. [PubMed: 30711343]
14. Lee SC; Knowles TJ; Postis VL; Jamshad M; Parslow RA; Lin YP; Goldman A; Sridhar P; Overduin M; Muench SP; Dafforn TR, A method for detergent-free isolation of membrane proteins in their local lipid environment. Nat. Protoc 2016, 11, 1149–62. [PubMed: 27254461]
15. Dörr JM; Koorengevel MC; Schäfer M; Prokofyev AV; Scheidelaar S; van der Cruijsen EAW; Dafforn TR; Baldus M; Killian JA, Detergent-free isolation, characterization, and functional reconstitution of a tetrameric K+ channel: The power of native nanodiscs. Proc. Natl. Acad. Sci. U.S.A 2014, 111, 18607–18612. [PubMed: 25512535]

16. Overduin M; Esmaili M, Structures and Interactions of Transmembrane Targets in Native Nanodiscs. SLAS DISCOVERY: Advancing Life Sciences R&D 2019, 2472555219857691.
17. Hall SCL; Tognoloni C; Charlton J; Bragginton EC; Rothnie AJ; Sridhar P; Wheatley M; Knowles TJ; Arnold T; Edler KJ; Dafforn TR, An acid-compatible co-polymer for the solubilization of membranes and proteins into lipid bilayer-containing nanoparticles. Nanoscale 2018, 10, 10609–10619. [PubMed: 29845165]
18. Ravula T; Hardin NZ; Ramadugu SK; Ramamoorthy A, pH Tunable and Divalent Metal Ion Tolerant Polymer Lipid Nanodiscs. Langmuir 2017, 33, 10655–10662. [PubMed: 28920693]
19. Yasuhara K; Arakida J; Ravula T; Ramadugu SK; Sahoo B; Kikuchi JI; Ramamoorthy A, Spontaneous Lipid Nanodisc Fomation by Amphiphilic Polymethacrylate Copolymers. J. Am. Chem. Soc 2017, 139, 18657–18663. [PubMed: 29171274]
20. Ravula T; Hardin NZ; Ramadugu SK; Cox SJ; Ramamoorthy A, Formation of pH-Resistant Monodispersed Polymer-Lipid Nanodiscs. Angew. Chem. Int. Ed. Engl 2018, 57, 1342–1345. [PubMed: 29232017]
21. Ravula T; Ramadugu SK; Di Mauro G; Ramamoorthy A, Bioinspired, Size-Tunable Self-Assembly of Polymer-Lipid Bilayer Nanodiscs. Angew. Chem. Int. Ed. Engl 2017, 56, 11466–11470. [PubMed: 28714233]
22. Oluwole A; Danielczak B; Meister A; Babalola J; Vargas C; Keller S, Solubilization of Membrane Proteins into Functional Lipid-Bilayer Nanodiscs Using a Diisobutylene/Maleic Acid Copolymer. Angew. Chem. Int. Ed. Engl 2017, 56, 1919–1924. [PubMed: 28079955]
23. Hardin NZ; Ravula T; Mauro GD; Ramamoorthy A, Hydrophobic Functionalization of Polyacrylic Acid as a Versatile Platform for the Development of Polymer Lipid Nanodisks. Small 2019, 15, e1804813. [PubMed: 30667600]
24. Fiori MC; Jiang Y; Altenberg GA; Liang H, Polymer-encased nanodiscs with improved buffer compatibility. Sci Rep 2017, 7, 7432. [PubMed: 28785023]
25. Hardin NZ; Kocman V; Di Mauro GM; Ravula T; Ramamoorthy A, Metal-Chelated Polymer Nanodiscs for NMR Studies. Angew Chem Int Ed Engl 2019, 58, 17246–17250. [PubMed: 31529579]
26. Ravula T; Kim J; Lee DK; Ramamoorthy A, Magnetic Alignment of Polymer Nanodiscs Probed by Solid-State NMR Spectroscopy. Langmuir 2020, 36, 1258–1265. [PubMed: 31961695]
27. Burridge KM; Harding BD; Sahu ID; Kearns MM; Stowe RB; Dolan MT; Edelmann RE; Dabney-Smith C; Page RC; Konkolewicz D; Lorigan GA, Simple Derivatization of RAFT-Synthesized Styrene-Maleic Anhydride Copolymers for Lipid Disk Formulations. Biomacromolecules 2020, 21, 1274–1284. [PubMed: 31961664]
28. Sun C; Gennis RB, Single-particle cryo-EM studies of transmembrane proteins in SMA copolymer nanodiscs. Chem Phys Lipids 2019, 221, 114–119. [PubMed: 30940443]
29. Ravula T; Hardin NZ; Ramamoorthy A, Polymer nanodiscs: Advantages and limitations. Chem Phys Lipids 2019, 219, 45–49. [PubMed: 30707909]
30. Dominguez Pardo JJ; van Walree CA; Egmond MR; Koorengevel MC; Killian JA, Nanodiscs bounded by styrene-maleic acid allow trans-cis isomerization of enclosed photoswitches of azobenzene labeled lipids. Chem Phys Lipids 2019, 220, 1–5. [PubMed: 30779906]
31. Dominguez Pardo JJ; Dorr JM; Renne MF; Ould-Braham T; Koorengevel MC; van Steenbergen MJ; Killian JA, Thermotropic properties of phosphatidylcholine nanodiscs bounded by styrene-maleic acid copolymers. Chem Phys Lipids 2017, 208, 58–64. [PubMed: 28923687]
32. Danielczak B; Meister A; Keller S, Influence of Mg(2+) and Ca(2+) on nanodisc formation by diisobutylene/maleic acid (DIBMA) copolymer. Chem Phys Lipids 2019, 221, 30–38. [PubMed: 30876867]
33. Overduin M; Esmaili M, Memtein: The fundamental unit of membrane-protein structure and function. Chem Phys Lipids 2019, 218, 73–84. [PubMed: 30508515]
34. Bada Juarez JF; Harper AJ; Judge PJ; Tonge SR; Watts A, From polymer chemistry to structural biology: The development of SMA and related amphipathic polymers for membrane protein extraction and solubilisation. Chem Phys Lipids 2019, 221, 167–175. [PubMed: 30940445]

35. Guo R; Sumner J; Qian S, Structure of Diisobutylene Maleic Acid Copolymer (DIBMA) and Its Lipid Particle as a “Stealth” Membrane-Mimetic for Membrane Protein Research. ACS Applied Bio Materials 2021.
36. Pantelopulos GA; Straub JE; Thirumalai D; Sugita Y, Structure of APP-C991–99 and implications for role of extra-membrane domains in function and oligomerization. Biochim Biophys Acta Biomembr 2018, 1860, 1698–1708. [PubMed: 29702072]
37. Overduin M; Wille H; Westaway D, Multisite interactions of prions with membranes and native nanodiscs. Chem Phys Lipids 2021, 236, 105063. [PubMed: 33600804]
38. Krishnarjuna B; Ravula T; Ramamoorthy A, Detergent-free extraction, reconstitution and characterization of membrane-anchored cytochrome-b5 in native lipids. Chem Commun (Camb) 2020, 56, 6511–6514. [PubMed: 32462144]
39. Sahoo BR; Genjo T; Moharana KC; Ramamoorthy A, Self-Assembly of Polymer-Encased Lipid Nanodiscs and Membrane Protein Reconstitution. J Phys Chem B 2019, 123, 4562–4570. [PubMed: 31050900]
40. Sahoo BR; Genjo T; Bekier M; Cox SJ; Stoddard AK; Ivanova M; Yasuhara K; Fierke CA; Wang Y; Ramamoorthy A, Alzheimer’s amyloid-beta intermediates generated using polymer-nanodiscs. Chem Commun (Camb) 2018, 54, 12883–12886. [PubMed: 30379172]
41. Smith AAA; Autzen HE; Faust B; Mann JL; Muir BW; Howard S; Postma A; Spakowitz AJ; Cheng YF; Appel EA, Lipid Nanodiscs via Ordered Copolymers. Chem 2020, 6, 2782–2795.
42. Adao R; Cruz PF; Vaz DC; Fonseca F; Pedersen JN; Ferreira-da-Silva F; Brito RMM; Ramos CHI; Otzen D; Keller S; Bastos M, DIBMA nanodiscs keep alpha-synuclein folded. Biochim Biophys Acta Biomembr 2020, 1862, 183314. [PubMed: 32304757]
43. Hothersall JD; Jones AY; Dafforn TR; Perrior T; Chapman KL, Releasing the technical ‘shackles’ on GPCR drug discovery: opportunities enabled by detergent-free polymer lipid particle (PoLiPa) purification. Drug Discov Today 2020, 25, 1944–1956.
44. Santoro SA, Identification of a 160,000 Dalton Platelet Membrane-Protein That Mediates the Initial Divalent Cation-Dependent Adhesion of Platelets to Collagen. Cell 1986, 46, 913–920. [PubMed: 3757029]
45. Zilly FE; Halemani ND; Walrafen D; Spitta L; Schreiber A; Jahn R; Lang T, Ca2+ induces clustering of membrane proteins in the plasma membrane via electrostatic interactions. EMBO J 2011, 30, 1209–20. [PubMed: 21364530]
46. Vannam R; Sayilgan J; Ojeda S; Karakyriakou B; Hu E; Kreuzer J; Morris R; Herrera Lopez XI; Rai S; Haas W; Lawrence M; Ott CJ, Targeted degradation of the enhancer lysine acetyltransferases CBP and p300. Cell Chem Biol 2021.
47. Ghazarian H; Hu W; Mao A; Nguyen T; Vaidehi N; Sligar S; Shively JE, NMR analysis of free and lipid nanodisc anchored CEACAM1 membrane proximal peptides with Ca(2+)/CaM. Biochim Biophys Acta Biomembr 2019, 1861, 787–797. [PubMed: 30639287]
48. Katti S; Nyenhuis SB; Her B; Cafiso DS; Igumenova TI, Partial Metal Ion Saturation of C2 Domains Primes Synaptotagmin 1-Membrane Interactions. Biophys J 2020, 118, 1409–1423. [PubMed: 32075747]
49. Li S; Du L; Tsona NT; Wang W, The interaction of trace heavy metal with lipid monolayer in the sea surface microlayer. Chemosphere 2018, 196, 323–330. [PubMed: 29310068]
50. Aleman EA; Lamichhane R; Rueda D, Exploring RNA folding one molecule at a time. Curr Opin Chem Biol 2008, 12, 647–54. [PubMed: 18845269]
51. Kotaka M; Gover S; Vandeputte-Rutten L; Au SW; Lam VM; Adams MJ, Structural studies of glucose-6-phosphate and NADP+ binding to human glucose-6-phosphate dehydrogenase. Acta Crystallogr D Biol Crystallogr 2005, 61, 495–504. [PubMed: 15858258]
52. Findeisen F; Minor DL Jr., Structural basis for the differential effects of CaBP1 and calmodulin on Ca(V)1.2 calcium-dependent inactivation. Structure 2010, 18, 1617–31. [PubMed: 21134641]
53. Karp ES; Tiburu EK; Abu-Baker S; Lorigan GA, The structural properties of the transmembrane segment of the integral membrane protein phospholamban utilizing (13)C CPMAS, (2)H, and REDOR solid-state NMR spectroscopy. Biochim Biophys Acta 2006, 1758, 772–80. [PubMed: 16839519]

54. Oxenoid K; Chou JJ, The structure of phospholamban pentamer reveals a channel-like architecture in membranes. Proc Natl Acad Sci U S A 2005, 102, 10870–5. [PubMed: 16043693]
55. Ghimire H; Abu-Baker S; Sahu ID; Zhou A; Mayo DJ; Lee RT; Lorigan GA, Probing the helical tilt and dynamic properties of membrane-bound phospholamban in magnetically aligned bicelles using electron paramagnetic resonance spectroscopy. Biochim Biophys Acta 2012, 1818, 645–50. [PubMed: 22172806]
56. Pathuri P; Vogeley L; Luecke H, Crystal structure of metastasis-associated protein S100A4 in the active calcium-bound form. J Mol Biol 2008, 383, 62–77. [PubMed: 18783790]
57. Radoicic J; Park SH; Opella SJ, Macrodiscs Comprising SMALPs for Oriented Sample Solid-State NMR Spectroscopy of Membrane Proteins. Biophys. J 2018, 115, 22–25. [PubMed: 29914645]
58. Prosser RS; Hwang JS; Vold RR, Magnetically Aligned Phospholipid Bilayers with Positive Ordering: A New Model Membrane System. Biophysical Journal 1998, 74, 2405–2418. [PubMed: 9591667]
59. Prosser RS; Hunt SA; DiNatale JA; Vold RR, Magnetically Aligned Membrane Model Systems with Positive Order Parameter: Switching the Sign ofSzzwith Paramagnetic Ions. Journal of the American Chemical Society 1996, 118, 269–270.
60. Ravula T; Ramamoorthy A, Magnetic Alignment of Polymer Macro-Nanodiscs Enables Residual-Dipolar-Coupling-Based High-Resolution Structural Studies by NMR Spectroscopy. Angewandte Chemie International Edition 2019, 58, 14925–14928. [PubMed: 31310700]
61. Ravula T; Sahoo BR; Dai X; Ramamoorthy A, Natural-abundance (17)O NMR spectroscopy of magnetically aligned lipid nanodiscs. Chem Commun (Camb) 2020, 56, 9998–10001. [PubMed: 32724998]
62. Prestegard JH; Bougault CM; Kishore AI, Residual Dipolar Couplings in Structure Determination of Biomolecules. Chemical Reviews 2004, 104, 3519–3540. [PubMed: 15303825]
63. Tjandra N; Bax A, Direct measurement of distances and angles in biomolecules by NMR in a dilute liquid crystalline medium. Science 1997, 278, 1111–4. [PubMed: 9353189]
64. Salmon L; Bascom G; Andricioaei I; Al-Hashimi HM, A general method for constructing atomic-resolution RNA ensembles using NMR residual dipolar couplings: the basis for interhelical motions revealed. J Am Chem Soc 2013, 135, 5457–66. [PubMed: 23473378]
65. Lange OF; Lakomek NA; Fares C; Schroder GF; Walter KF; Becker S; Meiler J; Grubmuller H; Griesinger C; de Groot BL, Recognition dynamics up to microseconds revealed from an RDC-derived ubiquitin ensemble in solution. Science 2008, 320, 1471–5. [PubMed: 18556554]
66. Di Mauro GM; La Rosa C; Condorelli M; Ramamoorthy A, Benchmarks of SMA-Copolymer Derivatives and Nanodisc Integrity. Langmuir 2021, 37, 3113–3121. [PubMed: 33645999]
67. Raffard G; Steinbruckner S; Arnold A; Davis JH; Dufourc EJ, Temperature–Composition Diagram of Dimyristoylphosphatidylcholine–Dicaproylphosphatidylcholine “Bicelles” Self-Orienting in the Magnetic Field. A Solid State2H and 31P NMR Study. Langmuir 2000, 16, 7655–7662.
68. Brindley AJ; Martin RW, Effect of divalent cations on DMPC/DHPC bicelle formation and alignment. Langmuir 2012, 28, 7788–96. [PubMed: 22548306]
69. Grushin K; White MA; Stoilova-McPhie S, Reversible stacking of lipid nanodiscs for structural studies of clotting factors. Nanotechnology Reviews 2017, 6, 139–148.
70. Ravula T; Barnaba C; Mahajan M; Anantharamaiah GM; Im SC; Waskell L; Ramamoorthy A, Membrane environment drives cytochrome P450’s spin transition and its interaction with cytochrome b5. Chem Commun (Camb) 2017, 53, 12798–12801. [PubMed: 29143058]
71. Martinez D; Decossas M; Kowal J; Frey L; Stahlberg H; Dufourc EJ; Riek R; Habenstein B; Bibow S; Loquet A, Lipid Internal Dynamics Probed in Nanodiscs. Chemphyschem 2017, 18, 2651–2657. [PubMed: 28573816]
72. Rodriguez Camargo DC; Korshavn KJ; Jussupow A; Raltchev K; Goricanec D; Fleisch M; Sarkar R; Xue K; Aichler M; Mettenleiter G; Walch AK; Camilloni C; Hagn F; Reif B; Ramamoorthy A, Stabilization and structural analysis of a membrane-associated hIAPP aggregation intermediate. Elife 2017, 6, e31226. [PubMed: 29148426]
73. Sahoo BR; Bekier ME 2nd; Liu Z; Kocman V; Stoddard AK; Anantharamaiah GM; Nowick J; Fierke CA; Wang Y; Ramamoorthy A, Structural Interaction of Apolipoprotein A-I Mimetic

Peptide with Amyloid-beta Generates Toxic Hetero-oligomers. J Mol Biol 2020, 432, 1020–1034. [PubMed: 31866295]

74. Sahoo BR; Genjo T; Cox SJ; Stoddard AK; Anantharamaiah GM; Fierke C; Ramamoorthy A, Nanodisc-Forming Scaffold Protein Promoted Retardation of Amyloid-Beta Aggregation. J Mol Biol 2018, 430, 4230–4244. [PubMed: 30170005]
75. Srivastava AK; Pittman JM; Zerweck J; Venkata BS; Moore PC; Sachleben JR; Meredith SC, beta-Amyloid aggregation and heterogeneous nucleation. Protein Sci 2019, 28, 1567–1581. [PubMed: 31276610]
76. Pithadia AS; Lim MH, Metal-associated amyloid-beta species in Alzheimer's disease. Curr Opin Chem Biol 2012, 16, 67–73. [PubMed: 22366383]
77. Ramamoorthy A; Lim MH, Structural characterization and inhibition of toxic amyloid-beta oligomeric intermediates. Biophys J 2013, 105, 287–8. [PubMed: 23870249]
78. Cheignon C; Tomas M; Bonnefont-Rousselot D; Faller P; Hureau C; Collin F, Oxidative stress and the amyloid beta peptide in Alzheimer's disease. Redox Biol 2018, 14, 450–464. [PubMed: 29080524]

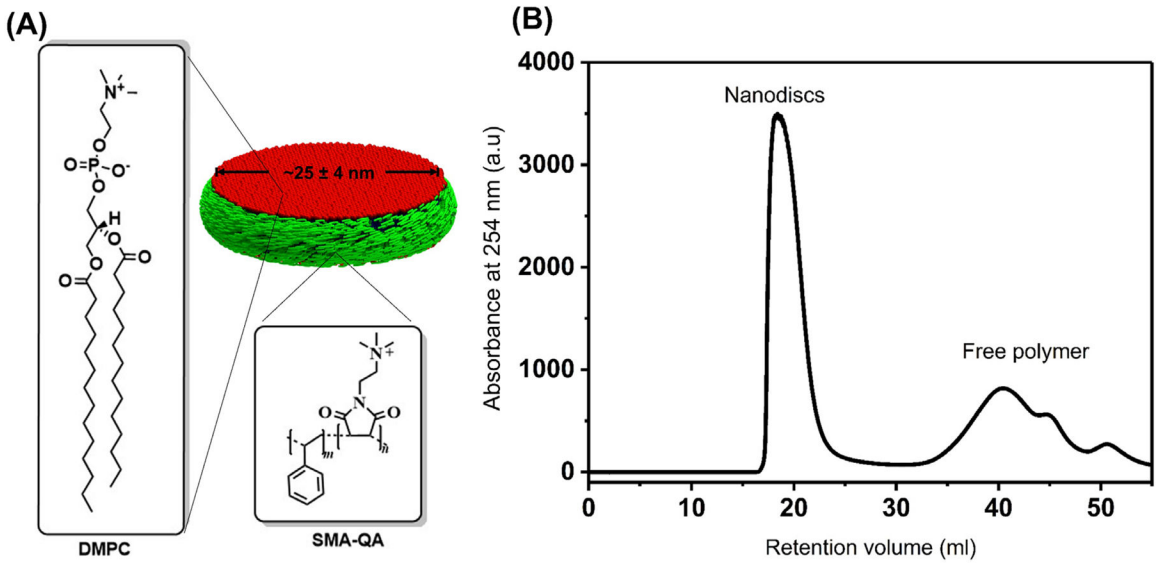


**Figure 1. Production and characterization of nanodiscs.**

(A) An illustration of SMA-QA based lipid nanodiscs used in this study. SMA-QA was synthesized from a styrene maleic anhydride polymer that has a ~1.3:1 molar ratio of styrene:maleic anhydride with $M_n$ = ~1.6 kDa. A desired polymer:lipid ratio is mixed to self-assemble to form the nanodiscs. Then, the nanodiscs are purified through size exclusion chromatography (SEC) to remove the free polymer and characterized using dynamic light scattering and NMR experiments. (B) SEC profile showing the elution volumes for the SMA-QA based lipid-nanodiscs and the free-(or aggregated) polymers from the sample. The first peak around 20 ml shows the overall size of nanodiscs and the relatively narrow width indicates the size uniformity of the nanodiscs. The second peak centered around 40 ml is from the free polymer aggregates that are not part of the nanodiscs in the sample. The interval between the two peaks assures the purity of nanodiscs sample as the free polymers can be removed from nanodiscs.

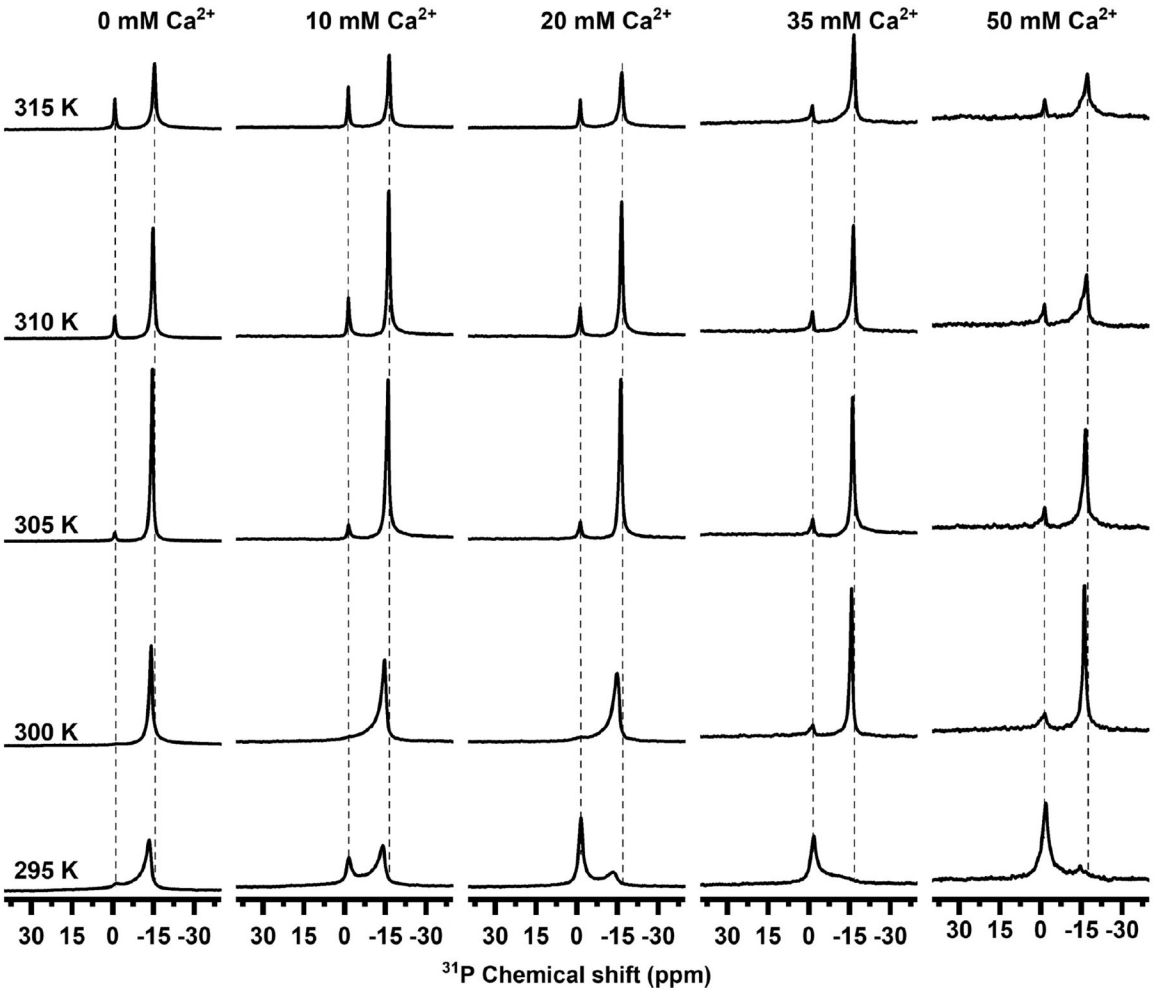


**Figure 2. Magnetic-alignment of macro-nanodiscs in the presence of $Ca^{2+}$ ions.**

Phosphorus-31 NMR spectra of magnetically-aligned 0.5:1 (w/w) SMA-QA:DMPC macro-nanodiscs with the lipid-bilayer-normal oriented perpendicular to the external magnetic field direction. Spectra were recorded on a 400 MHz Bruker solid-state NMR spectrometer at the indicated temperatures by varying the concentration of $Ca^{2+}$ ions as shown. Spectra obtained at 295 K have contributions from isotropic, anisotropic powder pattern, and anisotropic aligned lipid components. Simulation was used to quantify the individual components for the experimental spectrum obtained at 295 K with 10 mM $Ca^{2+}$ ions as shown in Figure S1 in the Supporting Information.

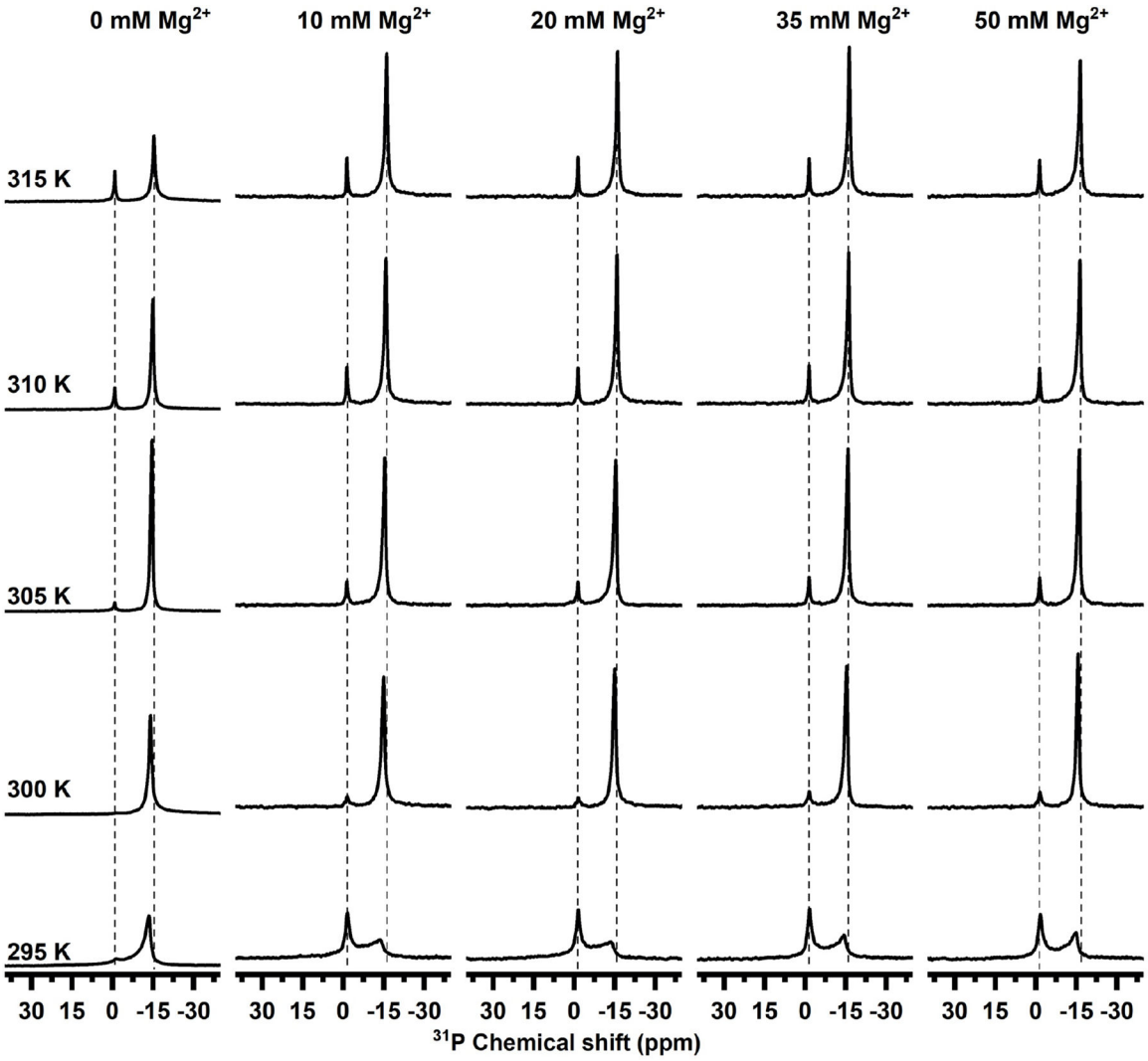


**Figure 3. Magnetic-alignment of macro-nanodiscs in the presence of $Mg^{2+}$ ions.**

Phosphorus-31 NMR spectra of magnetically-aligned 0.5:1 (w/w) SMA-QA:DMPC macro-nanodiscs with the lipid-bilayer-normal oriented perpendicular to the external magnetic field direction. Spectra were recorded on a 400 MHz Bruker solid-state NMR spectrometer at the indicated temperatures by varying the concentration of $Mg^{2+}$ ions as shown.

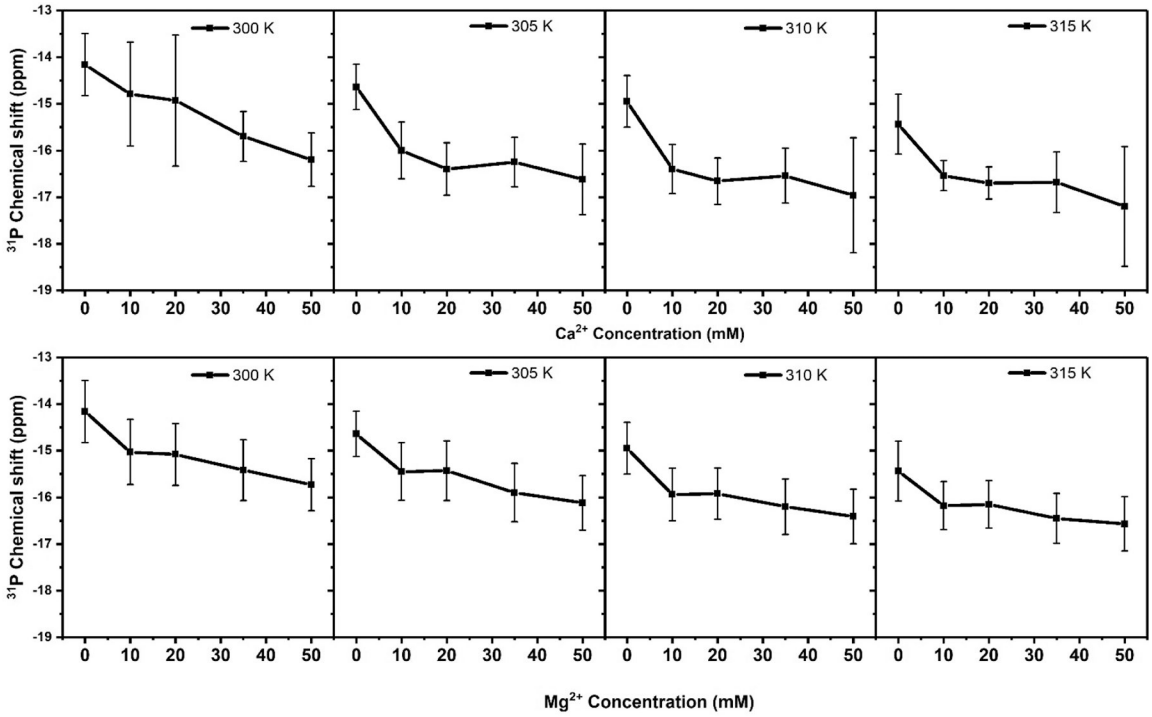


**Figure 4. Dependence of the extent of magnetic-alignment of nanodiscs on divalent metal ion concentration.**

Change in the $^{31}$P chemical shift frequency measured from magnetically-aligned 0.5:1 (w/w) SMA-QA:DMPC macro-nanodiscs, with the lipid-bilayer-normal oriented perpendicular to the external magnetic field direction, as a function of divalent metal ion concentration at the indicated temperature of the sample. Error bars represent the observed full-width at half-maximum from the respective $^{31}$P NMR spectrum.

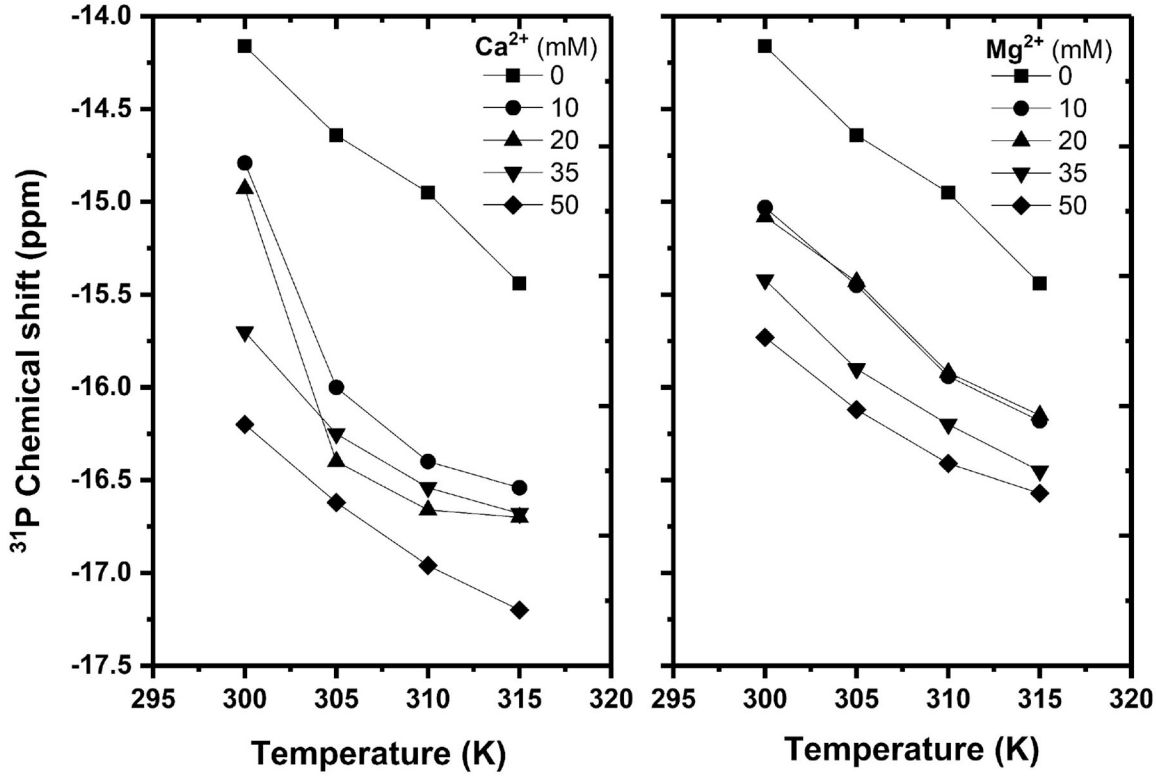


**Figure 5.**

Dependence of the extent of magnetic-alignment of nanodiscs on temperature. Change in the $^{31}$P chemical shift frequency measured from magnetically-aligned 0.5:1 (w/w) SMA-QA:DMPC macro-nanodiscs, with the lipid-bilayer-normal oriented perpendicular to the external magnetic field direction, as a function of temperature at the indicated divalent metal ion concentration: $Ca^{2+}$ (left) and $Mg^{2+}$ (right).

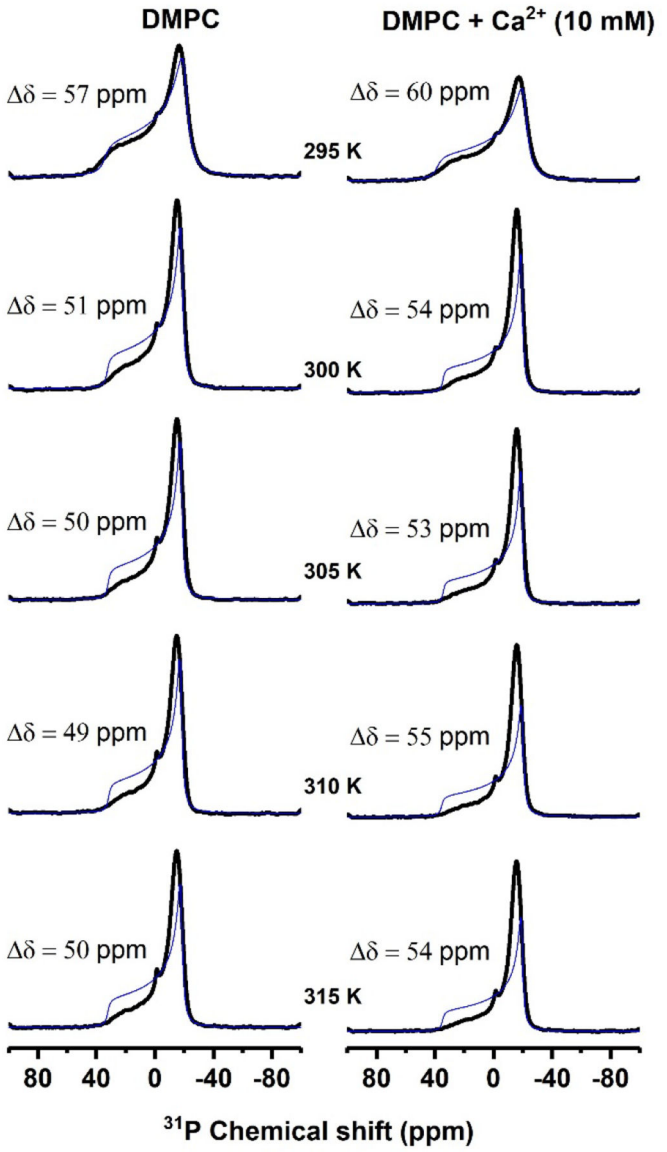


**Figure 6. Effect of calcium ions binding to lipids.**

$^{31}$P NMR spectra (experimental in black and simulated fit in blue) of DMPC multilamellar vesicles (MLVs) with and without 10 mM $Ca^{2+}$ ions obtained at the indicated sample temperature. $^{31}$P chemical shift anisotropy span, Δδ, was obtained by fitting the experimental spectra. The observed increase in the CSA span for $Ca^{2+}$-containing samples is due to $Ca^{2+}$ ions binding to lipids. The observed weak signal intensity near the parallel edge of the powder pattern (i.e. >20 ppm) may be due to calcium-ion-binding induced non-spherical distribution of lipids in MLVs.

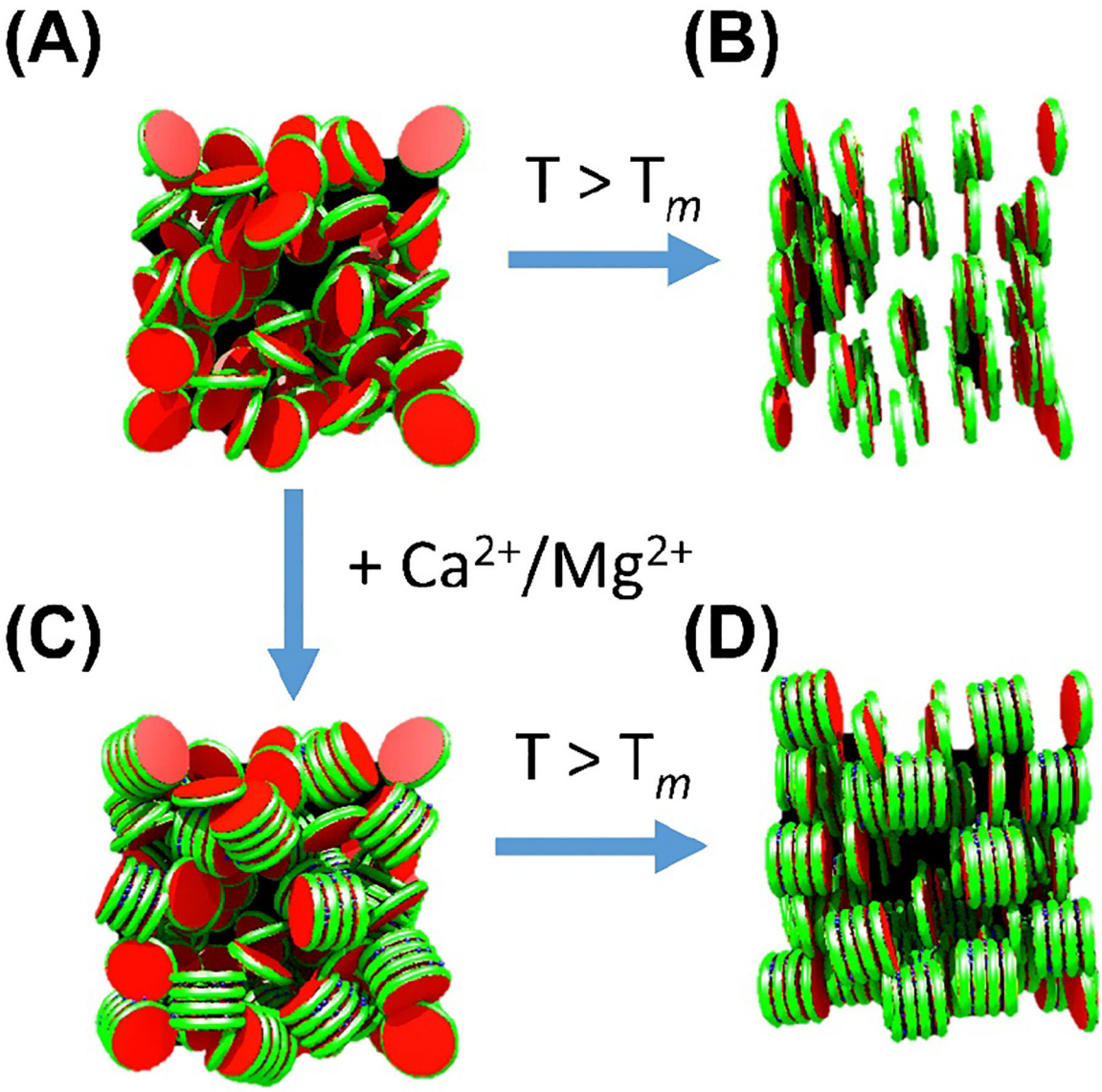


**Figure 7. Effect of calcium ions on the magnetic-alignment of nanodiscs.**

Illustration of: (A) the isotropic nature of polymer-based macro-nanodiscs below the main phase transition temperature ($T_m$) of the lipids present in the nanodiscs, (B) the anisotropic and magnetic-aligned state of the macro-nanodiscs above $T_m$, (C) the effect of $Ca^{2+}$ ions binding to lipid head-groups in stacking nanodiscs below Tm which result in a mixed phase that exhibits an anisotropic powder pattern and an isotropic $^{31}P$ peaks, and (D) the effect of $Ca^{2+}$ ions binding to lipids on the magnetic-alignment of stacked macro-nanodiscs above $T_m$.